Biochemical and Biophysical Research Communications 405 (2011) 303–307

Contents lists available at ScienceDirect

Biochemical and Biophysical Research Communications

journal homepage: www.elsevier.com/locate/ybbrc

A cell-death-defying factor, anamorsin mediates cell growth through inactivation of PKC and p38MAPK

Yuri Saito *, Hirohiko Shibayama, Hirokazu Tanaka, Akira Tanimura, Yuzuru Kanakura

Department of Hematology and Oncology, Osaka University Graduate School of Medicine, 2-2 Yamada-oka, Suita, Osaka 565-0871, Japan

ARTICLE INFO

Article history:
Received 5 January 2011
Available online 8 January 2011

Keywords:
Anamorsin
Cell proliferation
CyclinD1
PKC
p38MAPK

ABSTRACT

Anamorsin (AM) plays crucial roles in hematopoiesis and embryogenesis. AM deficient (AM KO) mice die during late gestation; AM KO embryos are anemic and very small compared to wild type (WT) embryos. To determine which signaling pathways AM utilizes for these functions, we used murine embryonic fibroblast (MEF) cells generated from E-14.5 AM KO or WT embryos. Proliferation of AM KO MEF cells was markedly retarded, and PKCθ, PKCδ, and p38MAPK were more highly phosphorylated in AM KO MEF cells. Expression of cyclinD1, the target molecule of p38MAPK, was down-regulated in AM KO MEF cells. p38MAPK inhibitor as well as PKC inhibitor restored expression of cyclinD1 and cell growth in AM KO MEF cells. These data suggest that PKCθ, PKCδ, and p38MAPK activation lead to cell cycle retardation in AM KO MEF cells, and that AM may negatively regulate novel PKCs and p38MAPK in MEF cells.

1. Introduction

Anamorsin (AM) (also called CIAPIN-1) is a cell-death-defying factor, which was originally isolated as a molecule that conferred resistance to apoptosis induced by growth factor starvation. AM is ubiquitously expressed in various organs, including hematopoietic tissues like bone marrow, spleen, and thymus. Expression of AM is also induced by various cytokines including SCF, EPO, and IL-3 through, at least partially, the Ras signaling pathway [1]. Besides apoptosis, AM is most likely involved in critical cellular processes such as development, growth, and differentiation [1–3]. AM-deficient mice die in late gestation. AM-deficient embryos are anemic and the size of the embryos is very small. It is thought that AM plays a crucial role in hematopoiesis during late and/or terminal stages of differentiation.

Expression of AM is also reported in several human solid tumors and hematological malignancies [4–7], such as hepatocellular carcinoma, gastric cancer, leukemia, and diffuse large B cell lymphoma. High levels of AM expression in cancer cells are associated with clinicopathological variables of tumor aggressiveness and may represent a prognostic marker of patient outcome [5–7].

The AM gene encodes an approximately 37 kDa protein. Bioinformatics analysis (PROSITE analysis) shows that AM is composed of a methyltransferase domain in the N-terminal region and a hypothetical Zn-ribbon-like motif in the C-terminal region [3]. AM is therefore implicated as an intracellular signaling molecule that may act via posttranslational modifications of cell-cycle-dependent proteins [8], however, precise biological effects of AM have not been fully elucidated yet.

To determine the signaling pathways involved, we used murine embryonic fibroblast (MEF) cells derived from AM-deficient embryos (AM KO-MEF) or wild type embryos (WT-MEF). Proliferation of AM KO-MEF cells was remarkably reduced when compared with that of WT-MEF cells. We examined activation states of signaling molecules in these cells, especially when stimulated with the PKC activator, PMA, and found that PKCθ, PKCδ and p38MAPK were more highly phosphorylated in AM KO MEF cells than in WT MEF cells. This study presents a novel mechanism that may elucidate the functions of AM.

2. Materials and methods

2.1. Cells and cell culture

Murine embryonic fibroblast (MEF) cells were isolated from E-14.5 mouse embryos and cultured in Dulbecco's modified Eagle's medium (DMEM) supplemented with 10% FCS and antibiotics (penicillin/streptomycin) at 37 °C in an atmosphere of 5% CO_2. MEF cells were expanded for two passages before use, then serum-starved for 24 h. Stimulation of cells was performed by addition of 20 nM PMA (Cell signaling) in DMSO for the indicated times.

2.2. Antibodies and inhibitors

Anti-ERK1/2, anti-ERK1/2(P), anti-Akt, anti-Akt(P), anti-NF-κB (p65), anti-NF-κB (p65)(P), anti-p38MAPK, anti-p38MAPK(P), anti-PKCθ(P), anti-PKCδ(P), anti-PKCα/β(P), anti-PKCζ/λ(P) and

* Corresponding author. Fax: +81 6 6879 3879.
E-mail address: saito-yu@bldon.med.osaka-u.ac.jp (Y. Saito).

0006-291X/$ - see front matter © 2011 Elsevier Inc. All rights reserved.
doi:10.1016/j.bbrc.2011.01.033

anti-cyclinD1 antibodies were purchased from Cell Signaling Technology, anti-β-actin antibody was purchased from Santa Cruz Biotechnology. Horseradish peroxidase (HRP)-labeled anti-mouse, anti-rabbit, and anti-goat secondary antibodies were purchased from Promega. The p38MAPK inhibitor, SB203580 and the PKC inhibitor, Rottlerin were obtained from Calbiochem. Rottlerin is known to be a specific inhibitor for novel PKCs [9]. IC_{50}(μM) value of Rottlerin for PKCθ and PKCδ was reported to be 3–6 μM.

2.3. Western blot analysis

Cell lysate samples were run on SDS–PAGE gel (PAGEL) (Atto Corporation), and then proteins in the gel were transferred to polyvinylidene fluoride (PVDF) membrane (Millipore). After membranes were blocked at RT for 1 h, they were washed in TBS-T before incubation with the first antibody overnight at 4 °C. Resulting membranes were incubated with secondary antibody conjugated to HRP for 30 min at RT and then developed using Western Lighting Chemiluminescence Reagent (PerkinElmer).

2.4. Cell proliferation assay

MEF cells were seeded in 6-well plates at 5×10^3 cells per well and cultured in DMEM with 10% FCS at 37 °C. The p38MAPK inhibitor, SB203580 and the PKC inhibitor, Rottlerin were added at a concentration of 10 μM and 3 μM, respectively. Cell proliferation was determined by counting the number of live cells using trypan blue (Invitrogen).

2.5. Quantitative RT-PCR assay

RT-PCR was performed as described previously [1]. Quantitative PCR was performed using a mixture of primer sets and probe, MA0353889-s1 for cyclin D1, MA00438064-A1 for cyclin A2, MA00487656-A1 for Mdm2, MA00468171-A1 for E2F-5 and MA99999915-g1 for GAPDH (ABI PRISM, Applied Biosystems).

2.6. cDNA microarray analysis

We performed a cDNA microarray analysis with GEArray Q series mouse cell cycle gene array. (SAbiosciences, http://www.sabiosciences.com/GEArrayservice.php). We compared expression levels of cell-growth or apoptosis related genes (87 genes) between AM KO MEF cells and WT MEF cells.

2.7. Statistics

Continuous data were reported with mean and standard deviation (SD). Statistical significance was analyzed by the *t*-test; statistically significant differences were denoted by $p < 0.05$.

3. Results

3.1. Phenotypes of AM KO MEF cells

Targeted deletion of the AM gene in mice causes embryonic death. AM KO embryos are anemic and quite small when compared to WT embryos of the same age. To clarify the biological effects of AM, we compared MEF cells produced from AM KO or WT embryos. The proliferation of AM KO MEF cells was markedly reduced compared with that of WT MEF cells (Fig. 1A). Next, to determine the difference in expression levels of cell-growth or apoptosis related genes and the phosphorylation states of signaling molecules in these cells, we used cDNA microarray analysis to compare AM KO MEF cells with WT MEF cells (Supplementary Table 1). Among 87 cell-growth or apoptosis related genes, levels of cyclinD1 (0.52), cyclinB2 (0.57), cyclinB1 (0.67), MAD2 (0.69), p18 (0.71), and cyclinA2 (0.74) were significantly down-regulated in AM KO MEF cells, while levels of E2F-5 (1.78) and Mdm2 (1.61) were significantly up-regulated. Ratios of expression of other genes were between 0.75 and 1.5. We also found that levels of cyclinD1 mRNA (Fig. 1B) and protein (Fig. 1C) in AM KO MEF cells were down-regulated when compared with those of WT MEF cells. Moreover, phosphorylation of p38MAPK was enhanced in AM KO MEF cells compared to WT MEF cells (Fig. 1D).

3.2. Phosphorylation states of signal transduction molecules stimulated with PKC activator, PMA

The proliferation of anamorsin KO MEF cells was significantly reduced and we investigated the phosphorylation states of various molecules related to cell-growth or apoptosis when stimulated with PKC activator, PMA using Western blot analysis. P38MAPK was more phosphorylated in AM KO MEF cells than in WT MEF cells after stimulation with PMA (Fig. 2B), whereas ERK1/2, Akt, and NF-kB, JNK were phosphorylated at similar levels (Fig. 2A). Moreover, PKCθ, PKCδ (novel PKCs) were also more phosphorylated in AM KO MEF cells than in WT MEF cells although PKCα/β (conventional PKCs) and PKCζ/λ (atypical PKCs) were similarly phosphorylated (Fig. 2C).

3.3. Effects of inhibitors on AM KO MEF cells

We first performed a cell proliferation assay by adding the p38MAPK inhibitor, SB203580 to AM KO MEF cells to confirm whether the phosphorylation state of p38MAPK is related to growth retardation in AM KO MEF cells. Proliferation of AM KO MEF cells was partially restored by SB203580 and the level of cyclinD1 mRNA was up-regulated (Fig. 3A and B). Next, to investigate whether p38MAPK activation in AM KO MEF cells is mediated by PKCθ and PKCδ, we used the PKC inhibitor, Rottlerin on AM KO MEF cells and found that proliferation of AM KO MEF cells was also partially restored by Rottlerin and the level of cyclinD1 mRNA was up-regulated (Fig. 3C and D). Furthermore, we added Rottlerin on serum-starved AM KO MEF cells for 12 h prior to PMA stimulation then analyzed the phosphorylation state of p38MAPK. p38MAPK was inactivated by Rottlerin, showing that PKCs mediate p38MAPK phosphorylation in AM KO MEF cells (Fig. 4).

4. Discussion

AM was originally identified to be an anti-apoptosis molecule, but it is now known to play other essential roles in cell differentiation, organ development, cellular stress response, and surveillance checkpoints [1–3]. AM shows no homology to the apoptosis regulatory molecules of the Bcl-2 family, caspase family, IAP family, or other signal transduction molecules. It has a methyltransferase domain and a hypothetical Zn-ribbon-like motif, however, the precise mechanisms of AM functions were not elucidated. Since the body of AM deficient embryos is small compared with that of wild type littermates, we focused on mouse embryonic fibroblast (MEF) cells. The proliferation of AM KO MEF cells was quite retarded compared with that of WT MEF cells. Signal transduction in response to extracellular stimuli such as mitogen-activated protein kinase (MAPK) in many cell types is essential for regulation of cellular differentiation, proliferation and death [10]. It is well known that p38MAPK, stress-activated MAPK, is linked to cell differentiation, growth inhibition, apoptosis, and is also essential for survival in response to various stimuli [11]. Moreover, p38MAPK contributes to induction of the G1/S and G2/M check points, and also negatively

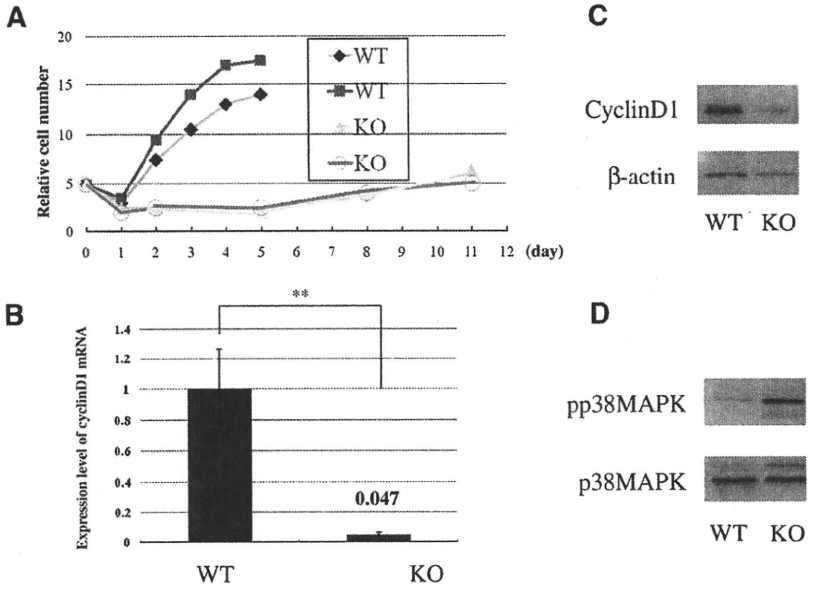

Fig. 1. Phenotypes of AM deficient (AM KO) MEF cells. The MEF cells were produced from E-14.5 AM KO embryos or wild type (WT) embryos. (A) Proliferation of AM KO MEF cells was significantly retarded compared with that of WT MEF cells. Cell number was determined by counting with trypan blue on the indicated days. (B, C) Expression levels of cyclinD1 was down-regulated in AM KO MEF cells. Cell extracts were prepared and subjected to quantitative RT-PCR assay and Western blot analysis using anti-cyclinD1 antibody. The histograms represent relative level of cyclinD1 mRNA (mean ± SD, $n = 3$). The p value is represented by asterisks (** $p < 0.01$). (D) p38MAPK was more phosphorylated in AM KO MEF cells than in WT MEF cells. Cell extracts were prepared and subjected to Western blot analysis with anti-phospho p38MAPK antibody or anti-p38MAPK antibody. (For interpretation of the references to colour in this figure legend, the reader is referred to the web version of this article.)

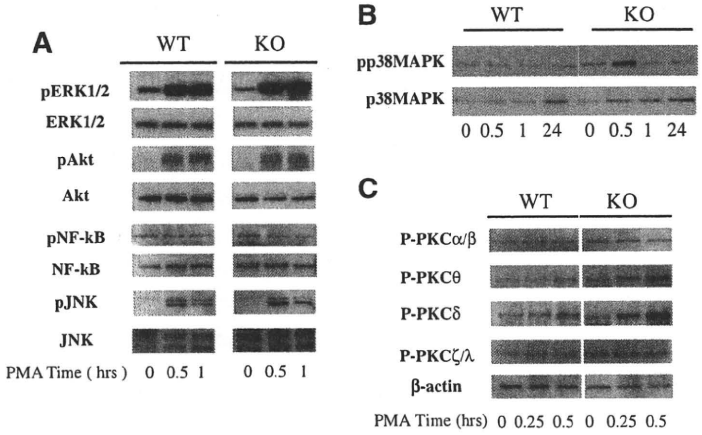

Fig. 2. AM negatively regulated p38MAPK, PKCθ, and PKCδ in stimulation with PKC activator, PMA. AM KO MEF cells or WT MEF cells were serum-starved for 24 h and stimulated with 20 nM PMA for the indicated times. Cell extracts were prepared and subjected to Western blot analysis with relevant antibodies. (A) Phosphorylation states of ERK1/2, Akt, NF-kB(p65), and JNK were similar between AM KO MEF cells and WT MEF cells. (B) The phosphorylation state of p38MAPK was more enhanced in AM KO MEF cells than in WT MEF cells. (C) Phosphorylation states of PKCθ and PKCδ (novel PKCs) were more enhanced whereas PKCα/β (conventional PKCs) and PKCζ/λ (atypical PKCs) were similarly phosphorylated in AM KO MEF cells compared with WT MEF cells.

regulates cyclinD1 expression [12]. The PKC family of intracellular serine/threonine kinases is also known to play critical roles in regulation of cellular differentiation and proliferation in many cell types [13]. The PKC family in mammals consists of 11 known members that are expressed in a wide variety of tissues and cell types. Based on sequence similarities, domain structures and cofactor requirements, PKC isoenzymes can be grouped into four structurally and functionally distinct subfamilies: (1) the Ca^{2+}-dependent conventional enzymes, consisting of PKCα, β and γ; (2) the Ca^{2+}-independent enzymes, termed as novel PKCs, consisting of PKCδ, ε, η, θ and μ; (3) atypical PKCs consisting of PKCζ and ι/λ; (4) PKC-related kinases (PKN) [14]. Among these PKC isoenzymes, we clarified that novel PKCs, especially PKCθ and PKCδ, were activated in AM KO MEF cells. We also examined phosphorylation of PKCα/β and PKCζ/λ and found that these conventional and atypical PKCs were not affected in AM KO MEF cells. Our data showed that PKCθ, PKCδ, and p38MAPK were more phosphorylated and that the expression level of cyclinD1 was down-regulated in AM KO MEF cells. PKC inhibitor blocked p38MAPK phosphorylation and p38MAPK inhibitor as well as PKC inhibitor restored expression of cyclinD1 and cell growth of AM KO MEF cells. Extrapolating from these data, we believe that PKCθ, PKCδ, and p38MAPK activation

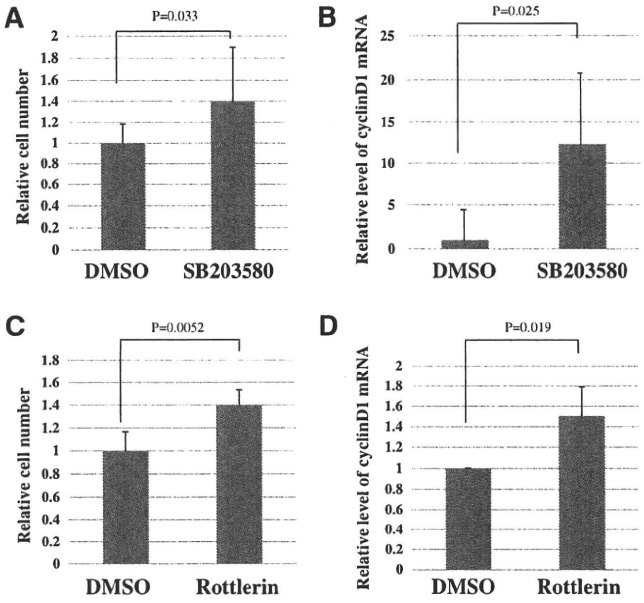

Fig. 3. PKCs and p38MAPK activation retarded proliferation of AM KO MEF cells. (A, C) An increase of cell number was observed in AM KO MEF cells treated with p38MAPK inhibitor, SB203580 and PKC inhibitor, Rottlerin. After treatment with each inhibitor for 3 days, cell numbers were determined using trypan blue. (B, D) SB203580 and Rottlerin up-regulated cyclinD1 mRNA expression in AM KO MEF cells. After 10 μM of SB203580 or 3 μM of Rottlerin was added to AM KO MEF cells for 24 h, cells were collected for RNA isolation. Expression level of cyclinD1 mRNA was examined by quantitative RT-PCR assay. The histograms represent relative level of cyclinD1 mRNA (mean ± SD, $n = 3$).

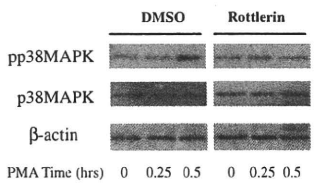

Fig. 4. Effect of PKC inhibitor, Rottlerin on phosphorylation state of p38MAPK in AM KO MEF cells. AM KO MEF cells were serum-starved for 24 h prior to treatment with 20 nM PMA for indicated times. For inhibition experiments, we added 3 μM of Rottlerin to the serum-starved cells for 12 h prior to PMA treatment. Western blot analysis was employed to analyze the phosphorylation state of p38MAPK. Rottlerin inhibited the phosphorylation of p38MAPK in AM KO MEF cells.

lead to cell cycle retardation in AM KO MEF cells and that AM might negatively regulate PKCθ, PKCδ, and p38MAPK in MEF cells. Although we here provide the results by using MEF cells, we will plan to analyze these mechanisms of AM function in other kinds of cells in future studies to determine whether AM works on PKCs other than novel PKCs. Hematopoiesis of AM KO embryos is obviously impaired. It will be interesting to learn whether the PKC–p38MAPK pathway works in hematopoietic cells from AM KO embryos in the same manner as in AM KO MEF cells. We also should clarify further mechanisms how AM regulate novel PKCs in future studies.

Our previous study and several other studies showed that AM was over-expressed in various kinds of solid tumors and hematological malignancies, and that high levels of AM were predictive of tumor progression and negative overall survival [4,7]. Another report showed that AM was over-expressed in multidrug resistant leukemic cells and gastric cancer [5,6]. Data from these studies suggest that AM might play crucial roles in oncogenesis. Recently, targeting oncogenes as novel cancer therapies has come into practical use [15,16]. Four kinds of strategies are used: (1) inhibition of oncogene expression through the use of molecular antagonists including antisense oligonucleotides, ribozymes and siRNA; (2) suppression of oncogene function using small-molecule inhibitors and peptidomimetics; (3) gene therapy based on the use of oncogene dominant-negative mutants or the application of oncogene promoters to drive expression of cytotoxic genes; and (4) immunotherapy. For AM, the first method has already been used in preclinical trials [4]. In our study, we found novel signaling pathways of AM functions and thought that suppression of oncogene function using small-molecule inhibitors and oncogene dominant-negative mutants may be promising as an AM targeted cancer therapy.

Research on AM has progressed significantly since our first report [1], however, the mechanisms of AM functions remain largely unknown. This study clarifies some of these mechanisms, although AM may act through other mechanisms as well. In order to understand this intriguing molecule more precisely, and to use these findings in clinical trials, further studies will be needed.

Acknowledgments

We thank Patricia Mantel for editing. This work was supported in part by grants from the Japanese Ministry of Education, Culture, Sports, Science and Technology, the Japanese Ministry of Health, Labor, and Welfare, and Mitsubishi Pharma Research Foundation.

Appendix A. Supplementary data

Supplementary data associated with this article can be found, in the online version, at doi:10.1016/j.bbrc.2011.01.033.

References

[1] H. Shibayama, E. Takai, I. Matsumura, M. Kouno, E. Morii, Y. Kitamuara, J. Takeda, Y. Kanakura, Identification of a cytokine-induced antiapoptotic molecule anamorsin essential for definitive hematopoiesis, J. Exp. Med. 199 (2004) 581–592.
[2] C. Mantel, Y. Guo, M.R. Lee, M.-K. Kim, M.-K. Han, H. Shibayama, S. Fukuda, M.C. Yoder, L.M. Pelus, K.-S. Kim, H.E. Broxmeyer, Checkpoint-apoptosis

uncoupling in human and mouse embryonic stem cells: a source of karyotypic instability, Blood 109 (2007) 4518–4527.
[3] X. Li, K. Wu, D. Fan, CIAPIN1 as a therapeutic target in cancer, Ther. Targets. 14 (2010) 1–8.
[4] X. Li, Y. Pan, R. Fan, H. Jin, S. Han, J. Liu, K. Wu, D. Fan, Adenovirus-delivered CIAPIN1 small interfering RNA inhibits HCC growth in vitro and in vivo, Carcinogenesis 29 (2008) 1587–1593.
[5] Z. Hao, X. Li, T. Qiao, R. Du, L. Hong, D. Fan, CIAPIN1 confers multidrug resistance by upregulating the expression of MDR-1 and MRP-1 in gastric cancer cells, Cancer Biol. Ther. 5 (2006) 261–266.
[6] X. Li, L. Hong, Y. Zhao, H. Jin, R. Fan, R. Du, L. Xia, G. Luo, D. Fan, A new apoptosis inhibitor, CIAPIN1 (cytokine-induced apoptosis inhibitor 1), mediates multidrug resistance in leukemia cells by regulating MDR-1, Bcl-2, and Bax, Biochem. Biochem. Cell Biol. 85 (2007) 741–750.
[7] T. Shizusawa, H. Shibayama, S. Murata, Y. Saitoh, Y. Sugimoto, I. Matsumura, H. Ogawa, H. Sugiyama, S. Fukuhara, M. Hino, A. Kanamara, A. Yamauchi, K. Aozasa, Y. Kanakura, The expression of anamorsin in diffuse large B cell lymphoma: possible prognostic biomarker for low IPI patients, Leuk. Lymphoma 49 (2008) 113–121.
[8] L. He, H. Wang, H. Jin, C. Guo, H. Xie, K. Yan, X. Li, Q. Shen, T. Qiao, G. Chen, N. Chai, L. Zhao, Q. Dong, Y. Zheng, J. Liu, D. Fan, CIAPIN1 inhibits the growth and proliferation of clear cell renal cell carcinoma, Cancer Lett. 276 (2009) 88–94.
[9] H. Sakai, M. Yamamoto, Y. Chiba, M. Misawa, Some different effect of PKC inhibitors on the acetylcholine, and endothelin-1 induced contractions of rat bronchial smooth muscle, Eur. J. Pharmacol. 618 (2009) 58–62.
[10] G. Pearson, F. Robinson, T.B. Gibson, B.-e. Xu, M. Karandikar, K. Berman, M.H. Cobb, Mitogen-activated protein (MAP) kinase pathways: regulation and physiological functions, Endocr. Rev. 22 (2001) 152–183.
[11] L.R. Coulthard, D.E. White, D.L. Jones, M.F. McDermott, S.A. Burchill, $p38^{MAPK}$: stress responses from molecular mechanisms to therapeutics, Trends Mol. Med. 15 (2009) 369–379.
[12] K. Page, J. Li, M.B. Hershenson, p38 MAP kinase negatively regulates cyclinD1 expression in airway smooth muscle cells, Am. J. Physiol. Lung Cell. Mol. Physiol. 280 (2001) L955–L964.
[13] M.R. Lee, W. Duan, S.-L. Tan, Protein kinase C isozymes as potential therapeutic targets in immune disorders, Expert Opin. Ther. Targets 12 (2008) 535–552.
[14] C. Rosse, M. Linch, S. Kermorgant, A.J.M. Cameron, K. Boeckeler, P.J. Parker, PKC and the control of localized signal dynamics, Nat. Rev. Mol. Cell Biol. 11 (2010) 103–112.
[15] T. Christoffersen, T.K. Guren, K.-L.G. Spindler, O. Dahl, P.E. Lonning, B.T. Gjertsen, Cancer therapy targeted at cellular signal transduction mechanisms: strategies, clinical results, and unresolved issues, Eur. J. Pharmacol. 625 (2009) 6–22.
[16] S. Ciavarella, A. Milano, F. Dammacco, F. Silvestris, Targeted therapies in cancer, Biodrugs 24 (2010) 77–88.

Journal of Medical Virology 83:317–321 (2011)

Epstein–Barr Virus in Diffuse Large B-Cell Lymphoma in Immunocompetent Patients in Japan is as Low as in Western Countries

Naoki Wada,[1] Junichiro Ikeda,[1] Yumiko Hori,[1] Shigeki Fujita,[1] Hiroyasu Ogawa,[2] Toshihiro Soma,[2] Haruo Sugiyama,[3] Shirou Fukuhara,[4] Akihisa Kanamaru,[5] Masayuki Hino,[6] Yuzuru Kanakura,[7] Eiichi Morii,[1] and Katsuyuki Aozasa[1]*

[1]*Department of Pathology, Osaka University Graduate School of Medicine, Suita, Osaka, Japan*
[2]*Department of Internal Medicine, Hyogo College of Medicine, Nishinomiya, Hyogo, Japan*
[3]*Department of Functional Diagnostic Science, Osaka University Graduate School of Medicine, Suita, Osaka, Japan*
[4]*First Department of Internal Medicine, Kansai Medical University, Moriguchi, Osaka, Japan*
[5]*Department of Hematology, Kinki University School of Medicine, Sayama, Osaka, Japan*
[6]*Department of Clinical Haematology and Diagnostics, Osaka City University Graduate School of Medicine, Osaka, Japan*
[7]*Department of Hematology and Oncology, Osaka University Graduate School of Medicine, Suita, Osaka, Japan*

According to previous reports, the frequency of Epstein–Barr virus (EBV) positivity in diffuse large B-cell lymphoma is higher in East Asia (approximately 9%) than in Western countries. The presence of the EBV genome was examined in diffuse large B-cell lymphoma patients registered with the Osaka Lymphoma Study Group (OLSG) in Osaka, Japan, situated in East Asia. The EBV-positive rate was examined with in situ hybridization (ISH) in 484 immunocompetent diffuse large B-cell lymphoma patients registered with OLSG. The male-to-female ratio was 1.29, with ages ranging from 16 to 95 (median, 68) years. ISH with EBV-encoded small RNAs (EBER) probes revealed positive signals in the nuclei of tumor cells: the frequency of positively stained cells among all tumor cells was almost none in 458 cases, 5–10% in 5, 10–20% in 5, 20–50% in 11, and >50% in 5. When the frequency was >20% or >50%, the EBV-positive rate in the present series (3.3% or 1.0%) was rather similar to that reported in Western cases. Careful evaluation of patient backgrounds, including age distribution, type of lymphomas, exclusion of immunocompromised patients, and establishment of definite criteria for EBV positivity (>20%, >50%, or almost all tumor cells) are essential in comparing geographical differences. ***J. Med. Virol. 83:317–321, 2011.*** © 2010 Wiley-Liss, Inc.

KEY WORDS: Epstein–Barr virus; diffuse large B-cell lymphoma; in situ hybridization; immunocompetence; geographical differences

INTRODUCTION

The Epstein–Barr virus (EBV), a γ-herpesvirus, is transmitted by mucosal secretions among the human population. An association between EBV and human lymphomas, including endemic Burkitt's lymphoma, Hodgkin lymphoma, and non-Hodgkin lymphomas of B-, T-, or NK-cell immunophenotypes, has been reported [Shah and Young, 2009]. In the recent WHO classification (2008), the chapter for EBV-positive diffuse large B-cell lymphoma of the elderly states that the EBV-positive rate in diffuse large B-cell lymphoma in Asian countries is 8–10% [Nakamura et al., 2008]. Hematologists and hematopathologists in the Osaka Lymphoma Study Group (OLSG) in Osaka, Japan, situated in the East Asia, felt a sense of incongruity for this figure, although they had no data on this.

Abbreviations: EBV, Epstein–Barr virus; OLSG, Osaka Lymphoma Study Group; LMP, latent membrane protein; ISH, in situ hybridization, EBER, EBV-encoded small RNAs; MTX, methotrexate; PNA, peptide nucleic acid; FITC, fluorescein isothiocyanate; DAB, 3,3′-diaminobenzidine tetrahydrochloride; CTL, cytotoxic T-lymphocytes.

We declare that we have no conflict of interest.

Grant sponsor: Ministry of Education, Science, Culture, Sports and Technology, Japan; Grant numbers: 20014012, 20590364, 20014010.

*Correspondence to: Katsuyuki Aozasa, MD, PhD, Department of Pathology (C3), Osaka University Graduate School of Medicine, 2-2 Yamadaoka, Suita, Osaka 565-0871, Japan.
E-mail: aozasa@molpath.med.osaka-u.ac.jp

Accepted 16 September 2010
DOI 10.1002/jmv.21967
Published online in Wiley Online Library (wileyonlinelibrary.com).

There have been two large-scale studies on the EBV positivity in diffuse large B-cell lymphoma from East Asian countries, one in Korea and one in Japan. Both studies showed a similar frequency of EBV positivity among diffuse large B-cell lymphoma, that is, 9% [Oyama et al., 2007; Park et al., 2007]. However, two points regarding these reports should be addressed. First, the age distribution was quite different between the Korean and Japanese cases: the percentage of cases older than 60 years was 36.6% in Korean and 60.6% in Japanese cases. It seems that the EBV-positive rate is higher in elder patients; thus, the difference in age distribution might affect EBV positivity. Second, the criteria for EBV positivity of diffuse large B-cell lymphoma was different: >20% of tumor cells with positive signals by in situ hybridization (ISH) in one report [Park et al., 2007] and >50% in another [Oyama et al., 2007]. Some Japanese investigators, adopting the criteria of almost all tumor cells with positive signals as EBV-positive, reported that 11.4% of their diffuse large B-cell lymphoma cases were EBV-positive [Kuze et al., 2000]. However, reports from Western countries apparently showed a much lower EBV-positive rate than did the East Asian ones [Gibson and Hsi, 2009; Hoeller et al., 2010]. Hoeller et al. [2010] reported that 10 (3.9%) of their 258 diffuse large B-cell lymphoma cases were EBV-positive: the percentage of positive cells was <20% in two cases, <50% in four, and >50% in four. Gibson and Hsi [2009] reported that none of their 90 diffuse large B-cell lymphoma, all older than 60 years, was EBV-positive. They stated that EBV-positive tumor cells were not identified in any of the 90 cases, and only three demonstrated very rare EBV-positive signals in small bystander lymphocytes (<1% of non-tumor cells).

In this study, we examined the presence of the EBV genome with ISH in the tumor cells in cases of diffuse large B-cell lymphoma registered with OLSG. The EBV-positive rate was then evaluated according to the criteria used in the previous and present studies, and the data were then compared with those reported from East Asia and Western countries in the light of clinical findings such as age, gender, and presence of immunodeficiencies.

MATERIALS AND METHODS

Patients

Between November 1999 and October 2009, in total, 4,490 cases were registered with the OLSG, Japan, in which 63 hospitals participate and register cases of malignant lymphomas and related conditions. All of the hematoxylin and eosin- and immunoperoxidase-stained sections were reviewed by one of the authors (K.A.) and classified according to the WHO classification. A diagnosis of malignant lymphoma was confirmed in 3,571 (79.5%) of 4,490 cases. Of these 3,571 cases, 3,273 (91.7%) were non-Hodgkin lymphoma and 298 (8.3%) were Hodgkin lymphoma. The number of diffuse large B-cell lymphoma cases was 1,590, which constituted 48.6% of all non-Hodgkin lymphoma. The latest 500 cases with diffuse large B-cell lymphoma registered during February 2007 to October 2009 were studied for the presence of the EBV genome. Most patients received anthracyclin-based chemotherapy and rituximab after the diagnosis. The numbers of patients who received excisional biopsy or surgical resection, punch biopsy, or needle biopsy were 384, 76, and 40, respectively. In cases receiving punch or needle biopsy, an adequate amount of material for histological analyses was obtained. The primary site was lymph node in 165 cases, extranodal organs in 204, and unknown in 131. Among them, two patients suffered from rheumatoid arthritis, one each from idiopathic thrombocytopenic purpura, interstitial pneumonia, Sjögren's syndrome, and uveitis, and were treated with prednisone, together with cyclosporine in one. These six cases were excluded for further analysis because of possible underlying immune abnormalities. During the same period, 14 cases of polymorphous lymphoproliferative disorders, 14 methotrexate (MTX)-associated lymphoproliferative disorders, five post-transplant lymphoproliferative disorders (liver, kidney, and cord blood in two, two, and one case, respectively), and one Hodgkin-like lymphoproliferative disorder were registered with the OLSG. Polymorphous lymphoproliferative disorders are defined as lymphoproliferative disorders showing a polymorphous pattern of proliferation, consisting of large lymphoid cells and various numbers of inflammatory cells [Nakamichi et al., 2010]. Polymorphous lymphoproliferative disorders usually affect individuals with a background of immunodeficiency. Clinical findings entered on the registration card for the OLSG included the following: name of hospital, age, gender, occupation, site of disease, clinical diagnosis, present illness, and peripheral blood and bone marrow findings, including differential counts, serum data, and chromosomal abnormalities of the tumor cells. History of medication (those receiving immunosuppressants) was also checked.

The Institutional Review Board for Clinical Research at Osaka University Hospital approved this study.

Immunohistochemistry

Antibodies used for immunohistochemistry were CD20, CD79a, CD3, CD30, and anti-Epstein–Barr virus/LMP/Clones CS. 1–4 (DakoCytomation, Glostrup, Denmark, diluted at 1:400, 1:100, 1:50, 1:25, and 1:100, respectively). Immunohistochemistry was performed using an automated staining system (Dako Autostainer, DakoCytomation).

In Situ Hybridization

ISH using the EBV-encoded small RNAs (EBER) probe was performed to examine the presence of the EBV genome in the formalin-fixed paraffin-embedded sections with the EBER DAB application kit (DakoCytomation). Briefly, sections were treated with proteinase K, diluted at 1:10 with TBS (50 mmol/L Tris–HCl buffered saline containing 150 mmol/L NaCl, pH 7.6), then hybridized with EBER PNA (peptide nucleic acid)

probe/fluorescein (DakoCytomation) at 55°C for 90 min. After blocking endogenous peroxidase activity, sections were incubated with rabbit anti-FITC (fluorescein isothiocyanate) antibody (1:50; Invitrogen, Carlsbad, CA) at room temperature for 30 min, incubated with ChemMate ENVISION/HRP polymer (DakoCytomation) at room temperature for 30 min, and colored with DAB (3,3′-diaminobenzidine tetrahydrochloride). This ISH method using an EBER probe was recently used in the author's laboratory. The EBV-positive rate in NK/T cell lymphoma by this method on paraffin-embedded sections was similar (80%) to that with the previously used method using an EBER-1 probe [Li et al., 2000].

The frequency of EBV positivity in the malignant large lymphoid cells was determined by averaging the number of positive cells from three high-power fields where the positive cells were larger in number. The tumors were then separated into five groups: tumors with almost no EBV positivity, tumors with 5–10%, 10–20%, 20–50%, and >50% of cells showing EBV positivity. According to the previous study, we adopted the criterion of >20% as EBV-positive.

Follow-Up

Adequate follow-up data was available in 16 EBV-positive and 204 EBV-negative diffuse large B-cell lymphoma cases. Follow-up periods for survivors in EBV-positive and -negative cases ranged from 5.2 to 38.5 (average 22.6) and 16.4–38.1 (average 25.5) months, respectively. Kaplan–Meier estimated survival rates at 2 and 3 years were calculated, and overall survival rates were compared by a log-rank test.

RESULTS

EBV-ISH was performed in 494 cases; however, informative data was not obtained in 10 cases because of specimen loss during staining procedures or severe non-specific staining of background/overstaining. As a result, staining results could be evaluated in only 484 cases. Positive signals were found in the nuclei of tumor cells: the frequency of positively stained cells among all tumor cells was almost none in 458 cases, 5–10% in 5, 10–20% in 5, 20–50% in 11, and >50% in 5 (Fig. 1).

Of 16 cases with >20% EBV-positive tumor cells (EBV-positive cases), large geographical necrosis was found in five cases. Angiotropism was not found. CD30 positivity was found in 6 of 15 EBV-positive cases. Tumor cells expressed latent membrane protein (LMP)-1 in 8 of 14 EBV-positive cases (Fig. 1).

In total, 40 cases with diffuse large B-cell lymphoma were excluded, due to the putative presence of immunocompromised conditions, including autoimmune diseases, receiving prednisone and cyclosporine, polymorphous lymphoproliferative disorders, MTX-associated lymphoproliferative disorders, post-transplant lymphoproliferative disorders, and Hodgkin-like lymphoproliferative disorders. The frequency of positively stained cells among all tumor cells was 20–50% in six cases and >50% in five.

The estimated survival rates at 2 and 3 years for the EBV-positive and -negative cases were 58.9% and 71.9% at 2 years and 58.9% and 69.0% at 3 years, respectively. The overall survival rates of the two groups were not statistically different (log-rank test; $P > 0.1$).

DISCUSSION

According to previous reports, frequency of EBV positivity in diffuse large B-cell lymphoma was higher in East Asia than in Western countries (Table I) [Kuze et al., 2000; Oyama et al., 2007; Park et al., 2007; Gibson and Hsi, 2009; Hoeller et al., 2010]. However, before accepting this, a careful evaluation of the data presented in the previous studies is necessary. Regarding clinical findings, the age distribution and gender ratio varied among these reports [Kuze et al., 2000; Oyama et al., 2007; Park et al., 2007; Gibson and Hsi, 2009; Hoeller et al., 2010]. A study referenced in the WHO classification adopting >50% of the criteria included cases of immunodeficiency-associated lymphomas, although the exact number was not shown. Lymphomas known to be closely associated with EBV infection such as pyothorax-associated lymphoma and Burkitt's lymphoma were also included [Oyama et al., 2007]. These procedures inevitably increased the EBV-positive rate of the study (13.6%). The routinely registered cases with the OLSG constitute the present series; thus, collection bias in the cases could be avoided. The age distribution and gender ratio in the present series are within the spectrum of the previously reported diffuse large B-cell lymphoma cases; thus, the present findings could be adopted as standard data.

The criteria for defining EBV-positive cases vary among the previous studies; >20% of the tumor cells in one study [Park et al., 2007] and >50% in another [Oyama et al., 2007]. In particular, a study from Japan adopting the criteria of almost all EBV-positive cells reported the EBV-positive rate to be 11.4% [Kuze et al., 2000]. When adopting >20% or >50% as EBV-positive, the EBV-positive rates among diffuse large B-cell lymphoma in immunocompetent hosts in the OLSG (3.3% or 1.0%) were rather similar to those in Western series [0–2.7%, 0–1.9%; Gibson and Hsi, 2009; Hoeller et al., 2010], but much lower than that in Korean (8.9%) [Park et al., 2007] and Japanese series (11.4–13.6%) [Kuze et al., 2000; Oyama et al., 2007].

The present and previous [Park et al., 2007; Gibson and Hsi, 2009; Hoeller et al., 2010] studies have analyzed the presence of the EBV genome in diffuse large B-cell lymphoma in immunocompetent patients. When a total of 40 cases with diffuse large B-cell lymphoma, which had been excluded from the calculation of the EBV-positive rate due to the putative presence of immunocompromised conditions (such as autoimmune disease, receiving prednisone and cyclosporine, polymorphous lymphoproliferative disorders, MTX-associated lymphoproliferative disorders, post-transplant lymphoproliferative disorders, and

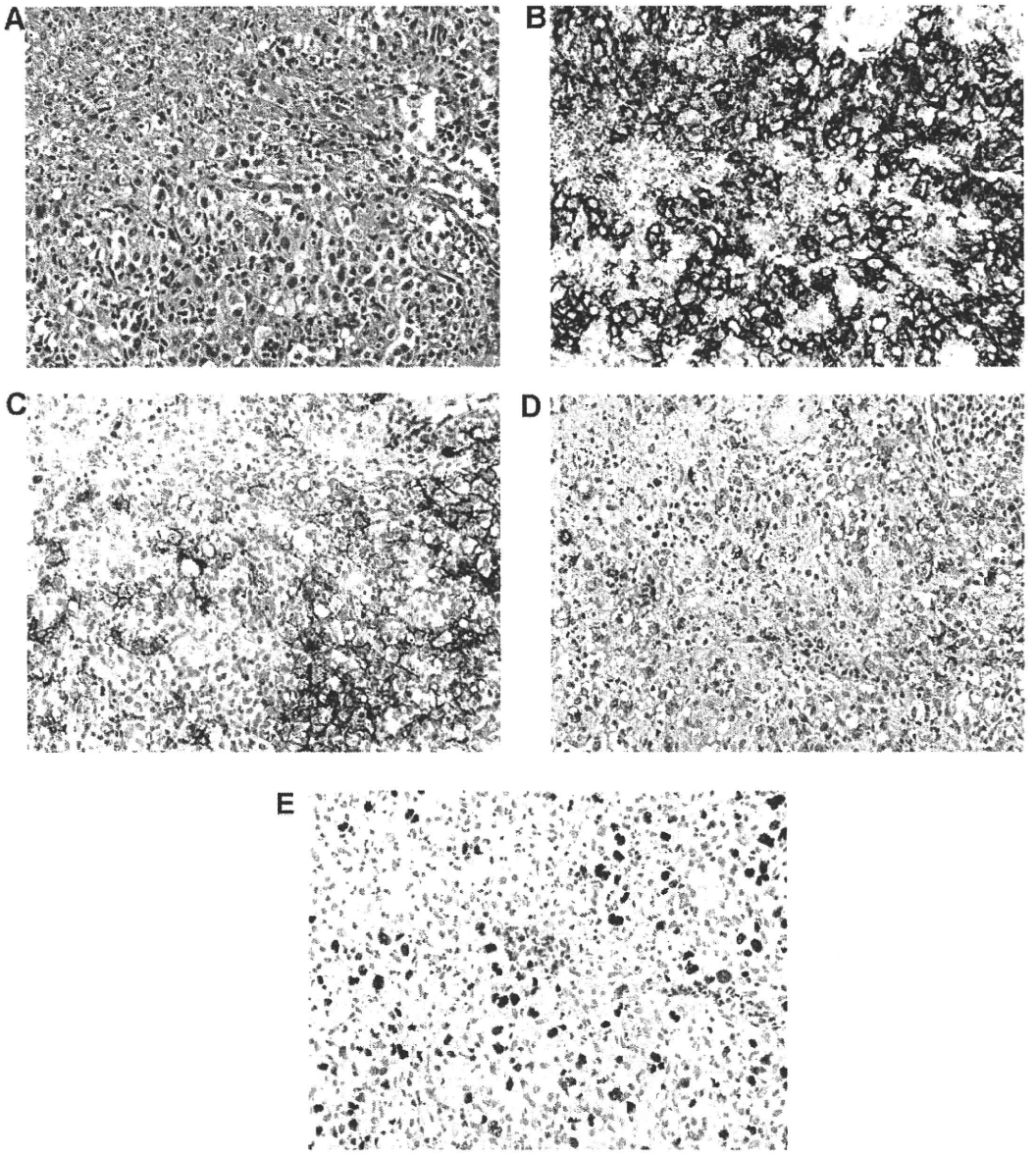

Fig. 1. **A**: Diffuse proliferation of large lymphoid cells with prominent nucleoli. H&E. Large lymphoid cells expressed CD20 (**B**) and less frequently CD30 (**C**), and LMP-1 (**D**). In situ hybridization with the EBER probe revealed positive signals in the nuclei of large lymphoid cells (**E**). All from the same case. Magnification: 400×.

Hodgkin-like lymphoproliferative disorders) were re-included in this study, the EBV-positive rate reached 5.2% or 1.9% using the >20% or >50% criteria, respectively.

The EBV genome has been detected in various kinds of malignant lymphomas, and latent infection genes of EBV, including LMP-1, show transforming activity in infected cells. LMP-1 serves as a target molecule for host cytotoxic T-lymphocytes (CTL); thus, B-lymphocytes expressing LMP-1 are recognized and eliminated by host CTL under normal immune conditions [Murray et al., 1992]. Of the present 14 EBV-positive cases, tumor cells expressed LMP-1 in eight.

Overall survival was reported to be significantly worse in EBV-positive diffuse large B-cell lymphoma cases than in EBV-negative cases [Oyama et al., 2007; Park et al., 2007]. In fact, this claim of a poor prognosis was one reason for incorporating the provisional entity, "EBV-positive diffuse large B-cell lymphoma of the elderly" (>50 years old), in the recently published textbook regarding the WHO classification (2008) [Nakamura et al., 2008]. In this study, however, overall survival rates of EBV-positive and -negative cases were not statistically different. In the present series from OLSG, about 90% of cases of diffuse large B-cell lymphoma were diagnosed at >50 years old. Two of 16 EBV-

TABLE I. Brief Clinical Findings and EBV-Positive Rate of Diffuse Large B-Cell Lymphoma in the Present and Reported Cases

		Western countries		East Asian countries		
	Present series (n = 484)	Switzerland, Italy, and Austria[a] (n = 341)	US[b] (n = 90)	Korea[c] (n = 380)	Japan[d] (n = 1,792)	Japan[e] (n = 114)
Age (years)						
Range (mean or median)	16–95 (mean: 67.0; median: 68)	M: 12–90 (mean: 64; median: 67) F: 18–93 (mean: 65; median: 67)	NA	18–95 (median: 56)	NA	11–89 (mean 64.1)
% of cases >50 years	89.7%	71.3%	NA	NA	80.5%	NA
% of cases >60 years	74.0%	NA	100%	36.6%	60.6%	NA
Sex ratio (M/F)	1.29	1.11	NA	1.39	NA	1.43
Immunologic abnormalities	Absent	Absent	Absent	Absent	Present in some cases[f]	NA
Criteria for EBV-positive rate (% among examined cases)						
≧5%	5.4%	NA	0%	NA	NA	NA
≧10%	4.3%	3.1%	0%	NA	NA	NA
≧20%	3.3%	2.7%	0%	8.9%	NA	NA
≧50%	1.0%	1.9%	0%	NA	13.6%	11.4%

NA, not available.
[a]Hoeller et al. [2010].
[b]Gibson and Hsi [2009].
[c]Park et al. [2007].
[d]Oyama et al. [2007].
[e]Kuze et al. [2000].
[f]Exact number was not shown.

positive cases were under 50 years old (38 and 27 years old).

In conclusion, this study revealed that EBV positivity in diffuse large B-cell lymphoma of immunocompetent patients in Japan is rather similar to that in Western countries. Careful evaluation of patient backgrounds and the adoption of common criteria for EBV positivity are essential in comparing geographical differences in EBV positivity in diffuse large B-cell lymphoma.

ACKNOWLEDGMENTS

We authors thank Ms. M. Tone, T. Sawamura, M. Sugano, and E. Maeno for technical assistance.

REFERENCES

Gibson SE, Hsi ED. 2009. Epstein–Barr virus-positive B-cell lymphoma of the elderly at a United States tertiary medical center: An uncommon aggressive lymphoma with a non-germinal center B-cell phenotype. Hum Pathol 40:653–661.

Hoeller S, Tzankov A, Pileri SA, Went P, Dirnhofer S. 2010. Epstein–Barr virus-positive diffuse large B-cell lymphoma in elderly patients is rare in Western populations. Hum Pathol 41:352–357.

Kuze T, Nakamura N, Hashimoto Y, Sasaki Y, Abe M. 2000. The characteristics of Epstein–Barr virus (EBV)-positive diffuse large B-cell lymphoma: Comparison between EBV(+) and EBV(−) cases in Japanese population. Jpn J Cancer Res 91:1233–1240.

Li T, Hongyo T, Syaifudin M, Nomura T, Dong Z, Shingu N, Kojya S, Nakatsuka S, Aozasa K. 2000. Mutations of the p53 gene in nasal NK/T-cell lymphoma. Lab Invest 80:493–499.

Murray RJ, Kurilla MG, Brooks JM, Thomas WA, Rowe M, Kieff E, Rickinson AB. 1992. Identification of target antigens for the human cytotoxic T cell response to Epstein–Barr virus (EBV): Implications for the immune control of EBV-positive malignancies. J Exp Med 176:157–168.

Nakamichi N, Wada N, Kohara M, Fukuhara S, Sugiyama H, Ogawa H, Hino M, Kanamaru A, Kanakura Y, Morii E, Aozasa K. 2010. Polymorphous lymphoproliferative disorder: A clinicopathological analysis. Virchows Arch 456:269–276.

Nakamura S, Jaffe ES, Swerdlow SH. 2008. EBV positive diffuse large B-cell lymphoma of the elderly. In: Swerdlow SH, et al., editors. WHO classification of tumours of haematopoietic and lymphoid tissues. 4th edition. World Health Organization classification of tumours. Lyon: IARC Press. pp. 243–244.

Oyama T, Yamamoto K, Asano N, Oshiro A, Suzuki R, Kagami Y, Morishima Y, Takeuchi K, Izumo T, Mori S, Ohshima K, Suzumiya J, Nakamura N, Abe M, Ichimura K, Sato Y, Yoshino T, Naoe T, Shimoyama Y, Kamiya Y, Kinoshita T, Nakamura S. 2007. Age-related EBV-associated B-cell lymphoproliferative disorders constitute a distinct clinicopathologic group: A study of 96 patients. Clin Cancer Res 13:5124–5132.

Park S, Lee J, Ko YH, Han A, Jun HJ, Lee SC, Hwang IG, Park YH, Ahn JS, Jung CW, Kim K, Ahn YC, Kang WK, Park K, Kim WS. 2007. The impact of Epstein–Barr virus status on clinical outcome in diffuse large B-cell lymphoma. Blood 110:972–978.

Shah KM, Young LS. 2009. Epstein–Barr virus and carcinogenesis: Beyond Burkitt's lymphoma. Clin Microbiol Infect 15:982–988.

Int J Hematol (2011) 93:106–111
DOI 10.1007/s12185-010-0731-5

CASE REPORT

Molecular analysis of a patient with type I Glanzmann thrombasthenia and clinical impact of the presence of anti-αIIbβ3 alloantibodies

Hirokazu Kashiwagi · Kazunobu Kiyomizu · Tsuyoshi Kamae · Tsuyoshi Nakazawa · Seiji Tadokoro · Shuji Takiguchi · Yuichiro Doki · Yuzuru Kanakura · Yoshiaki Tomiyama

Received: 28 October 2010 / Revised: 12 November 2010 / Accepted: 12 November 2010 / Published online: 8 December 2010

Abstract The occurrence of transfusion-related alloimmunization against αIIbβ3 is a major concern in patients with Glanzmann thrombasthenia (GT). However, few data are available about molecular defects of GT patients with anti-αIIbβ3 alloantibodies as well as clinical impact of these antibodies on platelet transfusion. Here, we report a case of type I GT with anti-HLA and anti-αIIbβ3 alloantibodies, who underwent laparoscopic total gastrectomy due to gastric cancer. We found a novel β3 nonsense mutation, 892C > T (Arg272X), and the patient was homozygous for the mutation. Laparoscopic gastrectomy was successfully performed with continuous infusion of HLA-matched platelet concentrates and bolus injection of recombinant factor VIIa at 2 h intervals. Total bleeding was 370 mL and no red-cell transfusion was necessary. Flow cytometric analysis employing anti-αIIbβ3 monoclonal antibody revealed that the transfused platelet count was maintained around 20–30 × 10^9/L during the operation and 10 × 10^9/L on the following day. Flow cytometric analysis also showed that transfused platelets retained normal reactivity to ADP stimulation. These results indicate that flow cytometry is useful to assess survival and function of transfused platelets in GT patients with anti-αIIbβ3 antibodies.

Keywords Glanzmann thrombasthenia · Anti-αIIbβ3 alloantibody · Mutation · Platelet transfusion · Recombinant factor VIIa

H. Kashiwagi · K. Kiyomizu · T. Kamae · T. Nakazawa · S. Tadokoro · Y. Kanakura · Y. Tomiyama
Department of Hematology and Oncology, Graduate School of Medicine, Osaka University, Suita, Osaka, Japan

S. Takiguchi · Y. Doki
Department of Gastroenterological Surgery, Graduate School of Medicine, Osaka University, Suita, Osaka, Japan

Y. Tomiyama (✉)
Department of Blood Transfusion, Osaka University Hospital, 2-15 Yamada-oka, Suita, Osaka 565-0871, Japan
e-mail: yoshi@hp-blood.med.osaka-u.ac.jp

1 Introduction

Glanzmann thrombasthenia (GT) is a rare hereditary bleeding disorder that is due to a quantitative and/or qualitative defect in integrin αIIbβ3 [glycoprotein (GP) IIb/IIIa, CD41/CD61]. GT is classified by the content of αIIbβ3: type I with <5% of normal controls, type II with 5–20%, and variant type with qualitative defect [1]. Clinical presentation includes mild to severe mucosal bleeds, traumatic or surgical hemorrhage, and occasional life-threatening bleeding episodes. Although treatment such as local measures and/or antifibrinolytics agents may be beneficial for mild bleeding, platelet transfusion is often necessary for severe bleeding, delivery and surgery. However, repeated transfusions may induce alloantibodies against HLA and/or αIIbβ3, leading to refractoriness to platelet transfusion. Moreover, it may be possible that anti-αIIbβ3 antibodies functionally block the binding of physiological ligands to αIIbβ3 on transfused platelets [2]. Treatment of GT patients with alloantibodies against αIIbβ3 are challenging. Removal of antibodies by plasma pheresis or immunoadsorption may be effective, although the procedure may present difficulties [3, 4]. In such cases, recombinant factor VIIa (rFVIIa) could represent an alternative. Tengborn and Petruson [5] reported the first successful case of rFVIIa treatment for epistaxes of a GT

patient, and Poon et al. [6] confirmed the effectiveness of rFVIIa to GT patients with international survey.

Despite clinical significance of anti-αIIbβ3 alloantibodies, little is known about genetic predisposing factors and the impact of anti-αIIbβ3 alloantibodies on the survival and function of transfused platelets in GT patients. We experienced a type I GT patient with anti-HLA and anti-αIIbβ3 antibodies suffering from gastric cancer, and laparoscopic total gastrectomy was successfully performed with HLA-matched platelet transfusion and bolus infusion of rFVIIa. In this study, we revealed a novel β3 mutation which could be responsible for the patient's phenotype and compared literally reported molecular defects of GT patients with anti-αIIbβ3 alloantibodies. Moreover, we assessed the survival and function of transfused normal platelets by monitoring of CD42b (GPIb) and αIIbβ3 expression employing flow cytometry.

2 Case report

A 59-year-old Japanese man was suffering from a lifelong bleeding tendency and diagnosed as GT. He was a son of consanguineous parents. He received several red-cell and platelet transfusions since his age of 51 due to gastrointestinal bleeding. He again noticed tarry stools in 2008 and consulted a hospital. Platelet transfusion was effective to make bleeding time normal at that time, and gastrointestinal fiberscope and endoscopic biopsy identified poorly differentiated adenocarcinoma at lesser curvature of the stomach body. However, after 2 months neither increase in platelet counts nor improvement of bleeding time was obtained even after high-dose γ-globulin administration followed by platelet transfusion, and the planned gastrectomy was cancelled. The patient was then referred to our hospital.

Employing several anti-αIIbβ3 monoclonal antibodies (mAbs), we confirmed that expression of αIIbβ3 on the patient's platelets was <5%, compared with that of normal controls, indicating that the patient was type I GT (Fig. 1A). To reveal a molecular genetic defect in this GT patient, we analyzed the whole coding region of αIIb and β3 cDNA amplified from platelet mRNA. A novel β3 nonsense mutation, 892C > T, which would lead to a premature termination of translation at arginine-272 residue of β3, was identified. Sequencing of exon 6 of the *ITGB3* gene, which is the corresponding exon of the 892C > T mutation, showed that he was homozygous for the mutation (Fig. 1B). Examination of the patient's plasma revealed that anti-HLA antibodies were positive in standard lymphocytotoxicity assay and immunofluorescence assay (data not shown). We also found that the patient's plasma antibodies apparently reacted with αIIbβ3-

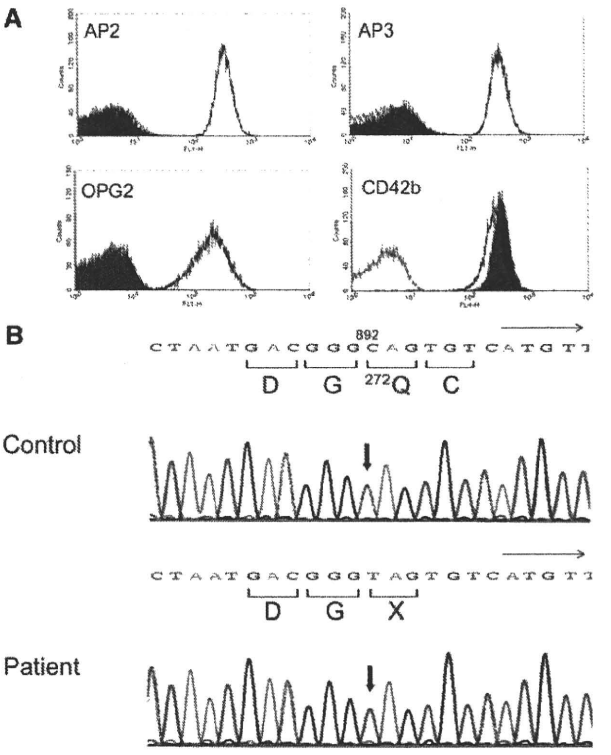

Fig. 1 Phenotype and molecular analysis of the GT patient. **A** Surface expression of glycoproteins on platelets. AP2, AP3 and OPG2 are αIIbβ3-specific, β3-specific and ligand-mimetic αIIbβ3-specific monoclonal antibodies, respectively. *Filled histograms* represent the patient's platelets. *Solid and dotted lines* represent control platelets and control IgG antibody, respectively. **B** Sequence analysis of exon 6 of the *ITGB3* gene. In the patient 892C was mutated to T, resulting in stop codon at the arginine-272 residue of β3

expressing 293 cells but not with untransfected 293T cells (Fig. 2A). Modified antigen-captured ELISA (MACE) assay [7] employing AP2, anti-αIIbβ3 mAb, as a capturing antibody clearly showed the presence of anti-αIIbβ3 antibodies as well (Fig. 2B). Therefore, we performed laparoscopic total gastrectomy under continuous infusion of two packs of HLA-matched apheresis-derived platelet concentrates containing 4.8×10^{11} and 3.5×10^{11} platelets with bolus infusion of 90 μg/kg of rFVIIa three times at 2 h intervals. The patient's platelet counts before, during, and just after the platelet transfusion were 150×10^9, 144×10^9, and 155×10^9/L, respectively, suggesting that transfused HLA-matched platelets were immediately destroyed by anti-αIIbβ3 antibodies. Then, we more precisely examined the survival of the transfused platelets employing flow cytometry. Transfused platelets were detected as CD41a (αIIbβ3) and CD42b double-positive cells, whereas autologous GT platelets were detected as CD41a-negative, CD42b-positive cells. As shown in Fig. 3A, CD41a-positive transfused platelets were 16.3 and 17.2% of total platelet counts during and just

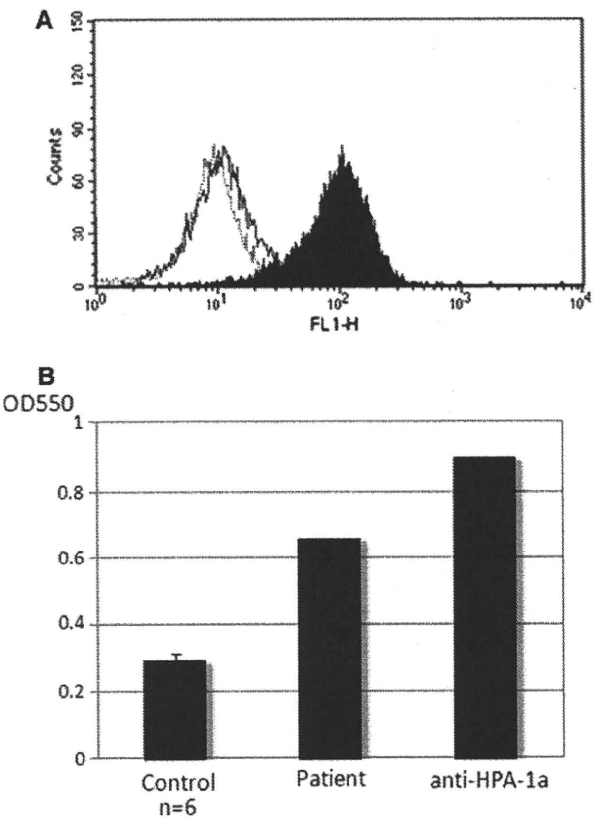

Fig. 2 Detection of anti-αIIbβ3 antibodies. **A** Plasma was incubated with αIIbβ3-stably expressed HEK293 cells. Bound IgG antibodies were detected by alexa488 anti-human IgG antibodies. *Filled and open histograms* represent the patient and normal control plasma, respectively. *Dotted line* represents the patient's plasma incubated with untransfected 293T cells. **B** Anti-αIIbβ3 antibodies were detected by MACE assay. Plasma was incubated with washed platelets obtained from blood type O subjects, and then lysed with 1% Triton X-100 buffer. Soluble fraction was added to AP2-coated microtiter well, and bound IgG was detected with biotin-conjugated anti-human IgG, followed by alkaline-phosphatase conjugated ABC kit (Vector Lab, Burlingame, CA, USA). Mean plus standard deviation of plasma obtained from 6 normal subjects is shown as negative controls. Anti-HPA-1a serum was used as positive control

after platelet transfusion, respectively. These data indicate that the numbers of the transfused platelets was estimated to 24×10^9 and 27×10^9/L (Fig. 3C). The ratio of survived CD41a-positive platelets decreased to 8.4% of total platelets on the next morning, indicating 10×10^9/L platelets were survived at that time. We also examined the function of the transfused platelets. Twenty micromolar ADP was added to the diluted whole blood samples simultaneously with FITC-PAC1, αIIbβ3 activation-dependent mAb, and PE-CD42b. The ratio of PAC1-bound platelets after ADP stimulation (13%) was comparable to that of CD41a-positive platelets (17%) during platelet transfusion, suggesting that function of the transfused platelets was not impaired by anti-αIIbβ3 alloantibodies in the patient's plasma (Fig. 3B). Although his hemoglobin concentration decreased from 14.1 to 11.0 g/dL after operation, total bleeding during the operation was 370 mL and no red-cell transfusion was necessary. Additional HLA-matched apheresis-derived platelet concentrate containing 3.0×10^{11} platelets was transfused on the following day. He was discharged after 2 weeks from the operation without any complication including bleeding.

3 Discussion

In GT patients, the occurrence of transfusion-related alloimmunization to αIIbβ3 is a major concern, as it results in the refractoriness to platelet transfusion. However, surprisingly few data are available concerning incidence, genetic factors and clinical impact of alloimmunization to αIIbβ3 in GT patients. Consistent with previous literature data that all patients with anti-αIIbβ3 alloantibodies are affected by type I GT [8, 9], our patient was type I. Although molecular basis of GT have been extensively analyzed, only seven mutations were reported in GT patients with anti-αIIbβ3 antibodies including our case [4, 9–12]. Interestingly, all patients are homozygote or compound heterozygote of premature termination mutations except one patient, who was a homozygote of β3(C575R) and produced anti-αIIbβ3 antibodies after massive platelet transfusion (Table 1). Santoro et al. [9] reported in the same literature that other two GT patients with β3(C575R) did not produce anti-αIIbβ3 antibodies after platelet transfusions. These results suggest that a mutation that causes a premature termination of translation could be a high risk for developing anti-αIIbβ3 alloantibodies. This hypothesis remains to be determined.

Effects of platelet transfusion are usually monitored simply by increase in platelet number. However, it might be difficult in case of surgery or massive bleeding, in which platelets are rapidly consumed physiologically. As reported previously [10, 13], in GT patients we can monitor survival of the infused platelets easily as αIIbβ3-positive cells by flow cytometry. Function of infused platelets might be also important, since anti-αIIbβ3 antibodies may interfere with ligand binding to αIIbβ3 [2]. Although bleeding time is usually used for monitoring platelet function, flow cytometric analysis using αIIbβ3 activation-dependent antibody, PAC-1, enabled us to assess the function of transfused platelets more easily and accurately [14]. In our case, despite that there was no increase of platelet counts after platelet transfusion, flow cytometric analysis revealed that αIIbβ3-positive platelets were maintained in 20–30 $\times 10^9$/L during the surgery and 10×10^9/L on the following day (Fig. 3C). Transfused platelets showed

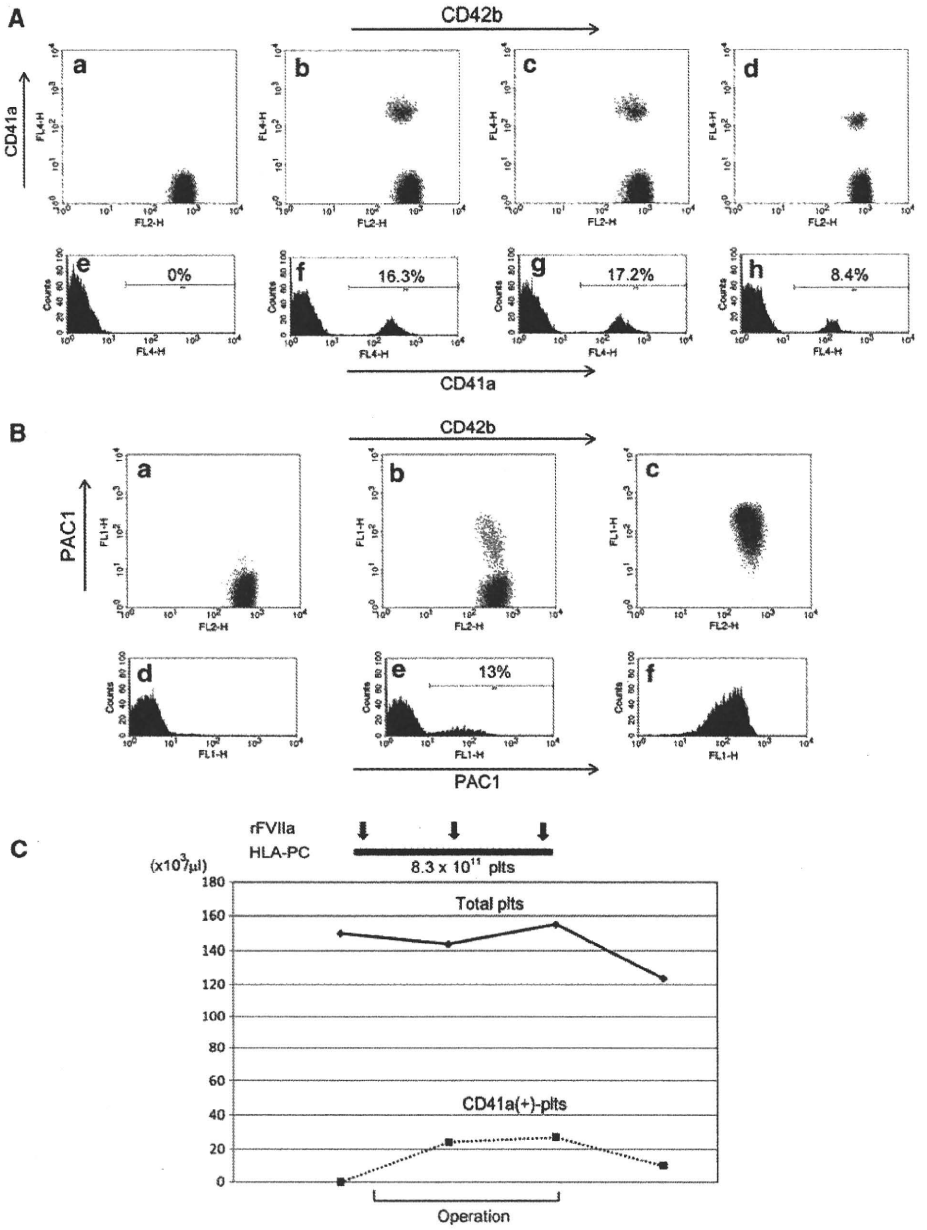

Fig. 3 Survival and function of the transfused normal platelets. **A** Detection of transfused platelets by flow cytometry. Whole blood cells diluted with Tyrodes buffer were mixed with APC-CD41a (HIP8; αIIbβ3-specific mAb) and PE-CD42b (GPIb) for 20 min. After fixed with 1% paraformaldehyde, two-color flow cytometric analysis was performed. *Upper panels* show PE-CD42b (*horizontal*)/APC-CD41a (*vertical*) dot blots. Transfused platelets were detected as CD42b(+)/CD41a(+). Lower panels show histograms of APC-CD41a and percentage of CD41a(+) platelets. *a*, *e* before operation, *b*, *f* during operation, *c*, *g* just after platelet transfusion, *d*, *h* 1-day post operation. **B** Detection of PAC1 binding after ADP stimulation. Twenty micromolar ADP was added to the diluted whole blood samples simultaneously with FITC-PAC1 and PE-CD42b. After 20 min incubation, the samples were fixed with paraformaldehyde, followed by flow cytometric analysis. *Upper panels* show PE-CD42b (*horizontal*)/FITC-PAC1 (*vertical*) dot blots and lower panels show histograms of FITC-PAC1. *a*, *d* During operation, no agonist. *b*, *e* During operation, 20 μM ADP (+). *c*, *f* Normal control, ADP (+). **C** Transition of total platelets counts and number of calculated CD41a-positive platelets. HLA-matched platelet concentrates containing 8.3×10^{11} platelets were transfused continuously during operation. Bolus infusion of 90 μg/kg of rFVIIa was done three times at 2 h intervals. *POD* post-operative day

normal response to ADP stimulation (Fig. 3B). These results suggest that transfused platelets could support primary hemostatic plug formation during and after surgery. However, it should be also mentioned that the increment of αIIbβ3-positive platelets was only 17% of predicted increase of platelet count after platelet transfusion,

Table 1 Reported mutations in GT patients with alloantibodies

Age and sex	Type	Mutations	Gene	αIIbβ3-Ab	HLA-Ab	
14, F	I	IVS15(+1)G > A (premature termination), homo	ITGA2B	Pos	Unknown	Martin et al. [4]
18, F	I	IVS2(−2)A > G (premature termination), homo	ITGB3	Pos	Unknown	Male et al. [10]
55, M	I	IVS15(+1)G > A (premature termination), homo	ITGA2B	Pos	Unknown	Dargaud et al. [11]
Unknown	I	Exon 3 premature termination, homo	ITGB3	Pos	Neg	Santoro et al. [9]
Unknown[a]	I	1801T > C (C575R), homo	ITGB3	Pos	Pos	Santoro et al. [9]
M	I	1413C > G (Y471X)/1882C > T (R628X), compound hetero	ITGA2B	Pos	Neg	Nurden et al. [12]
59, M	I	892C > T (Q272X), homo	ITGB3	Pos	Pos	Our case

[a] Developed antibodies after massive (160 units) platelet transfusions

suggesting that the transfused platelets were rapidly cleared by anti-αIIbβ3 antibodies as anticipated.

Effectiveness of rFVIIa for GT with anti-αIIbβ3 antibodies is first described by Tengborn and Petruson [5], and international survey confirms it [6]. Although the precise mechanism of action of rFVIIa on GT platelets is largely unknown, impairment of thrombin generation capacity in GT platelets has been demonstrated. Experimental evidences suggest that high-dose rFVIIa can bind to activated platelet surface, and promote thrombin generation via direct activation of FX to FXa, which is sufficient to convert fibrinogen to fibrin [15]. Despite the lack of αIIbβ3, GT platelets have been shown to agglutinate in the presence of fibrin, particularly polymeric fibrin via unidentified receptors on platelet surface [16]. Although we could not assess the efficiency of rFVIIa in our case because platelet transfusion was used simultaneously, the fact that in spite of poor increment of transfused platelets bleeding in the surgery was minimal suggests the effectiveness of rFVIIa.

In conclusion, we found a novel β3 mutation, leading a premature termination of translation, in a GT patient with anti-αIIbβ3 antibodies. We could also assess the impact of anti-αIIbβ3 antibodies by monitoring the survival and function of transfused platelets in surgery.

Acknowledgments This work was supported in part by Grant-in Aid for Scientific Research from the Ministry of Education, Culture, Sports, Science and Technology in Japan, from the Ministry of Health, Labor and Welfare in Japan; and "Academic Frontier" Project in Japan.

Conflict of interest There are no conflicts of interest.

References

1. Tomiyama Y. Glanzmann thrombasthenia: integrin αIIbβ3 deficiency. Int J Hematol. 2000;72:448–54.
2. Gruel Y, Brojer E, Nugent DJ, Kunicki TJ. Further characterization of the thrombasthenia-related idiotype OG. Antiidiotype defines a novel epitope(s) shared by fibrinogen B beta chain, vitronectin, and von Willebrand factor and required for binding to β3. J Exp Med. 1994;180:2259–67.
3. Ito K, Yoshida H, Hatoyama H, Matsumoto H, Ban C, Mori T, et al. Antibody removal therapy used successfully at delivery of a pregnant patient with Glanzmann's thrombasthenia and multiple anti-platelet antibodies. Vox Sang. 1991;61:40–6.
4. Martin I, Kriaa F, Proulle V, Guillet B, Kaplan C, D'Oiron R, et al. Protein A Sepharose immunoadsorption can restore the efficacy of platelet concentrates in patients with Glanzmann's thrombasthenia and anti-glycoprotein IIb–IIIa antibodies. Br J Haematol. 2002;119:991–7.
5. Tengborn L, Petruson B. A patient with Glanzmann thrombasthenia and epistaxis successfully treated with recombinant factor VIIa. Thromb Hemost. 1996;75:981–2.
6. Poon MC, D'Oiron R, Von Depka M, Khair K, Négrier C, Karafoulidou A, et al. International Data Collection on Recombinant Factor VIIa and Congenital Platelet Disorders Study Group. Prophylactic and therapeutic recombinant factor VIIa administration to patients with Glanzmann's thrombasthenia: results of an international survey. J Thromb Haemost. 2004;2:1096–103.
7. Kosugi S, Tomiyama Y, Honda S, Kato H, Kiyoi T, Kashiwagi H, et al. Platelet-associated anti-GPIIb-IIIa autoantibodies in chronic immune thrombocytopenic purpura recognizing epitopes close to the ligand-binding site of glycoprotein (GP) IIb. Blood. 2001;98:1819–27.
8. Bellucci S, Caen J. Molecular basis of Glanzmann's Thrombasthenia and current strategies in treatment. Blood Rev. 2002;16:193–202.
9. Santoro C, Rago A, Biondo F, Conti L, Pulcinelli F, Laurenti L, et al. Prevalence of allo-immunization anti-HLA and anti-integrin αIIbβ3 in Glanzmann Thrombasthenia patients. Haemophilia. 2010;16:805–12.
10. Male C, Koren D, Eichelberger B, Kaufmann K, Panzer S. Monitoring survival and function of transfused platelets in Glanzmann thrombasthenia by flow cytometry and thrombelastography. Vox Sang. 2006;91:174–7.
11. Dargaud Y, Bordet JC, Trzeciak MC, Vinciguerra C, Negrier C. A case of Glanzmann's thrombasthenia successfully treated with recombinant factor VIIa during a surgical procedure: observation on the monitoring and the mechanism of this drug. Haemotologica. 2006;91:58–61.
12. Nurden AT, Kunicki T, Nurden P, Fiore M, Martins N, Heilig R, et al. Mutation analysis for a patient with Glanzmann Thrombasthenia who produced a landmark alloantibody to the αIIbβ3 integrin. J Thromb Haemost. 2010;8:1866–8.
13. Nurden A, Combrie R, Nurden P. Detection of transfused platelets in a patient with Glanzmann thrombasthenia. Thromb Haemost. 2002;87:543–4.

14. Shattil SJ, Cunningham M, Hoxie JA. Detection of activated platelets in whole blood using activation-dependent monoclonal antibodies and flow cytometry. Blood. 1987;70:307–15.
15. Monroe DM, Hoffman M, Oliver JA, Roberts HR. Platelet activity of high-dose factor VIIa is independent of tissue factor. Br J Haematol. 1997;99:542–7.
16. Poon MC. Clinical use of recombinant human activated factor VII (rFVIIa) in the prevention and treatment of bleeding episodes in patients with Glanzmann's thrombasthenia. Vasc Health Risk Manag. 2007;3:655.

ARTICLE
Journal of Cellular Biochemistry 112:147–156 (2011)

Journal of Cellular Biochemistry

Identification of Functional Domains and Novel Binding Partners of STIM Proteins

Norimitsu Saitoh,[1] Kenji Oritani,[1*] Kazunobu Saito,[2,3] Takafumi Yokota,[1] Michiko Ichii,[1] Takao Sudo,[1] Natsuko Fujita,[1] Koichi Nakajima,[4] Masato Okada,[3] and Yuzuru Kanakura[1]

[1]*Department of Hematology and Oncology, Graduate School of Medicine, Osaka University, Osaka, Japan*

[2]*DNA-Chip Development Center for Infectious Diseases, Research Institute for Microbial Diseases, Osaka University, Osaka, Japan*

[3]*Department of Oncogene Research, Research Institute for Microbial Diseases, Osaka, University, Osaka University, Osaka, Japan*

[4]*Department of Immunology, Osaka City University Graduate School of Medicine, Osaka, Japan*

ABSTRACT

With a signal trap method, we previously identified stromal interaction molecule (STIM: originally named as SIM) as a protein, which has a signal peptide in 1996. However, recent works have accumulated evidences that STIM1 and STIM2 reside in endoplasmic reticulum (ER) and that both mainly sense ER Ca^{2+} depletion, which plays an essential role in store operated calcium entry. In the present study, we extensively analyzed the domain functions and associated molecules of STIMs. A STIM1 mutant lacking the coiled-coil domains was massively expressed on the cell surface while mutants with the coiled-coil domains localized in ER. In addition, STIM1 mutants with the coiled-coil domains showed a longer half-life of proteins than those without them. These results are likely to indicate that the coiled-coil domains of STIM1 are essential for its ER-retention and its stability. Furthermore, we tried to comprehensively identify STIM1-associated molecules with mass spectrometry analysis of co-immunoprecipitated proteins for STIM1. This screening clarified that both STIM1 and STIM2 have a capacity to bind to a chaperone, calnexin as well as two protein-transporters, exportin1 and transportin1. Of importance, our result that glycosylation on STIM1 was not required for the association between STIM1 and calnexin seems to indicate that calnexin might function on STIM1 beyond a chaperone protein. Further information concerning regulatory mechanisms for STIM proteins including the data shown here will provide a model of Ca^{2+} control as well as a useful strategy to develop therapeutic drugs for intracellular Ca^{2+}-related diseases including inflammation and allergy. J. Cell. Biochem. 112: 147–156, 2011.

KEY WORDS: STIM; ENDOPLASMIC RETICULUM; COILED-COIL; HALF LIFE; CALNEXIN

Changes of intracellular calcium (Ca^{2+}) levels provide universal signals, which regulate various cellular events, such as gene expression, secretion, and differentiation [Berridge et al., 2000, 2003]. In electrochemically non-excitable cells, endoplasmic reticulum (ER) acts to store an intracellular pool of Ca^{2+}, which is released soon after the activation of receptors for cytokines or hormones. In addition, Ca^{2+} depletion from ER leads to the rapid activation of plasma membrane Ca^{2+} channels in a process known as store-operated Ca^{2+} (SOC) entry [Putney, 1986, 2007]. This Ca^{2+} entry is essential for the refill of Ca^{2+} in ER and the cytokine/hormone-induced sustained increase of intracellular Ca^{2+} as well. Recent important findings in this area are the identification of stromal interaction molecule (STIM) and orai proteins; STIM1 and STIM2 as sensors of ER luminal Ca^{2+} changes and Orai1, Orai2, and Orai3 as components of highly Ca^{2+}-selective SOC channels [Liou et al., 2005; Roos et al., 2005; Vig et al., 2006; Zhang et al., 2006].

STIM1 and STIM2 are single-pass, type-I transmembrane proteins, which mainly localize in ER [Williams et al., 2001; Soboloff et al., 2006a; Stathopulos et al., 2008]. Both proteins contain a helix-tern-helix EF-hand Ca^{2+}-sensing domain followed by a sterile α motif (SAM) in luminal side of ER. In addition, their cytoplasmic segment has two stretches of the coiled-coil domains and a highly acidic stretch. Both STIM1 and STIM2 have been proposed to sense ER-luminal Ca^{2+} levels. Indeed, luminal Ca^{2+} depletion results in the redistribution of STIM1 from ER homogeneity to discrete "puncta" in close proximity to the plasma membrane where it can activate SOC channels [Zhang et al., 2005;

*Correspondence to: Dr. Kenji Oritani, MD, Department of Hematology and Oncology, Graduate School of Medicine, Osaka University, 2-2 Yamadaoka, Suita City, Osaka 565-0871, Japan. E-mail: oritani@bldon.med.osaka-u.ac.jp
Received 24 March 2010; Accepted 28 September 2010 • DOI 10.1002/jcb.22910 • © 2010 Wiley-Liss, Inc.
Published online 4 November 2010 in Wiley Online Library (wileyonlinelibrary.com).

Luik et al., 2006; Wu et al., 2006; Liou et al., 2007]. During this puncta formation, Ca^{2+} depletion induces the oligomerization of STIM1 through its EF-SAM regions [Stathopulos et al., 2008]. Its coiled-coil regions also mediate constitutive homotypic interactions, leading to the stabilization of the EF-SAM-triggered oligomers as well as the translocation of STIM1.

Although available information about biochemical and physiological properties of STIM proteins, little is known about the domain functions of STIMs and their association molecules, which could help us understand not only why STIMs can display their specific functions but also what molecules control the localization and protein content of STIMs in cells. In the present study, we have found that the coiled-coil domains of STIM1 are essential for its ER-localization and protein stabilization. In addition, we have identified calnexin, exportin1, and transportin1 as novel associated molecules of STIMs with mass spectrometry analysis of co-immunoprecipitated proteins for STIM1.

MATERIALS AND METHODS

PLASMID CONSTRUCTS

To produce FLAG-tagged STIM1 and its deletion mutants, mouse STIM1 cDNA was amplified by PCR using a F4-9/pEFBOS plasmid as a template [Oritani and Kincade, 1996]. The PCR primers are as follows: 5′-GGGGGATCCACCGTCATGGATGTGTGCGCC-3′ and 5′-TTCTTCGGAGAATTCTTCGAGCTCCCC-3′ for STIM1(Full), 5′-GGGGGATCCACCGTCATGGATGTGTGCGCC-3′ and 5′-GTACCGGATCTGTTCCGGGAGCTCCCC-3′ for STIM1(EX + TM + CC), 5′-GGGGGATCCACCGTCATGGATGTGTGCGCC-3′ and 5′-GTGTACTTCTTTTACTACGAGCTCCCC-3′ for STIM1(EX + TM), 5′-GGGGGATCCACCGTCATGGATGTGTGCGCC-3′ and 5′-TGAGCCGTATTAGTGGACGAGCTCGGG-3′ for STIM1(EX). Each PCR product was then digested with BamH1 and Xho1, and ligated into FLAG-pcDNA 3 expression vector (Addgene, Cambridge, MA) (STIM1(Full)-FLAG, STIM1(EX + TM + CC)-FLAG, STIM1(EX + TM)-FLAG, STIM1(TM)-FALG, respectively). In these constructs, a FLAG tag was inserted into C-terminal of each cDNA. For STIM2(Full)-FLAG, the plasmid was constructed in a similar way to STIM1 constructs by using pENTR11 mSTIM2 myc (Addgene) as a template and 5′-GGGGGATCCACGGAAACAATGAAC-3′ and 5′-TTCTTCTTCAGATTCGAGCTCGGG-3′ as primers. To produce STIM1 lacking two Asn-linked glycosylation sites (STIM1(delGly)-FLAG), site-directed mutagenesis was performed. To substitute two "Asn"s at positions 131 and 171 for "Ala"s, site-directed mutagenesis using STIM(Full)-FLAG as a template was performed. The PCR primersare as follows: 5′-GGGGGATCCACCGTCATGGATGTGTGCGCC-3′ and 5′-AGTCTTCACATGCGGACCTGACACCTA-3′ as well as 5′-TCAGAAGTGTACGCCTGGACTGTGGAT-3′ and 5′-TTCTTCGGAGAATTCTTCGAGCTCCCC-3′ for the substitution of N131A, 5′-GGGGGATCCACCGTCATGGATGTGTGCGCC-3′ and 5′-GATCGTCATTGGCGGTGGTGGTACTGT-3′ as well as 5′-CTAGCAGTAACCGCCACCACCATGACA-3′ and 5′-TTCTTCGGAGAATTCTTCGAGCTCCCC-3′ for the substitution of N171A. The final PCR product (primers: 5′-GGGGGATCCACCGTCATGGATGTGTGCGCC-3′ and 5′-TTCTTCGGAGAATTCTTCGAGCTCCCC-3′) was digested with BamH1 and Xho1, and ligated into FLAG-pcDNA3 expression vector. Nucleotide sequences of all constructs were verified by sequencing.

CELL CULTURE AND TRANSFECTION

A human embryonic kidney carcinoma cell line (293T) and a human cervix carcinoma cell line (HeLa) were cultured in Dubecco's modified Eagle's medium (DMEM); (Nacalai Tesque, Kyoto, Japan) supplemented with 10% fetal bovine serum (FBS); (Equitec-Bio, Kerrville, TX). STIM1-deficient DT40 B cell line, a kind gift from Dr. Baba and Dr. Kurosaki (Osaka University, Osaka, Japan), was cultured in RPMI (Nacalai Tesque) supplemented with 10% FBS, 1% chiken serum (Biowest, Nuaille, France), 2 mM L-glutamine, and 50 μM 2-Mercaptoethanol. Transient transfection of plasmids into 293T and HeLa cells was performed with Lipofectamine 2000 (Invitrogen, Carlsbad, CA) according to manufacturer protocols. Stable transfection into DT40 cells was performed with Amaxa (Amaxa Biosystems, Gaithersburg, MD) according to manufacturer protocols.

IMMUNOPRECIPITATION AND WESTERN BLOT

The immunoprecipitation and Western blotting assays were performed as described previously [Sekine et al., 2005]. In some experiments, the transfectants were lysed after their surface proteins were labeled with biotin (EZ-Link Sulfo-NHS-SS-Biotin; Pierce, Rockford, IL). The antibodies used in this study were listed as follows: ANTI-FLAG® M2-Agarose Affinity Gel (Sigma-Aldrich, St. Louis, MO), anti-FLAG antibody (Sigma), anti-STIM1 (Abnova, Taipei, Taiwan), anti-calnexin (Stressgen, Ann Arbor, MI), anti-exportin1 (Bethyl Laboratories, Montgomery, TX), anti-transportin1 (ImmuQuest, Cleveland, UK), and anti-calreticulin (Affinity BioReagents, Golden, CO) as well as anti-Mouse IgG HRP conjugate (Promega, Madison, WI), anti-Rabbit IgG HRP conjugate (Promega), and Streptavidin-HRP (Pierce).

CONFOCAL MICROSCOPY

After HeLa cells were transfected with the indicated plasmids, cell fixation, permeablization, and immunofluorescence staining was performed as described previously [Muromoto et al., 2006]. The following antibodies were used: mouse anti-FLAG antibody (Sigma), rabbit anti-PDI antibody (Cell Signaling, Danvers, MA) as well as Alexa Fluor® 568 goat anti-mouse IgG and Alexa Fluor® 488 goat anti-rabbit IgG (Invitrogen). The nuclei of cells were stained with DAPI (Invitrogen, Eugene, OR). The stained samples were visualized with LSM 5 PASCAL (Carl Zeiss, Tokyo, Japan) according to manufacturer protocols.

ANALYSIS OF PROTEIN STABILITY

Twenty-four hours after transient transfection with indicated plasmids, HeLa cells were plated out onto 24 well plates. The cells were starved for 5 h in 500 μl of cysteine and methionine free medium (Invitrogen) supplemented with 10% methionine free FBS (Sigma), pulse-labeled in 200 μCi/ml of ^{35}S-methionine (MP Biomedicals, Solon, OH) for 1 h. After rinsing with chase medium (DMED supplemented with 10% FBS and 20 mM methionine and 20 mM cysteine), the cells were cultured for 0, 1, 2, and 3 days. The cultured cells were lysed with lysis buffer and precipitated with ANTI-FLAG® M2-Agarose Affinity Gel (Sigma) for 4 h. The eluted proteins were separated by 5–20% SDS-polyacrylamide gels.

The gels were dried and autoradiographed with BAS-2500 (FUJIFILM, Tokyo, Japan). The radioactivity of each specific band was calculated using Image Gauge V4.22 (FUJIFILM) software.

CALCIUM MEASUREMENT

For Ca^{2+} measurement, 1×10^7 DT40 cells were incubated with 5 μM Fluo4-AM (Invitrogen) and 1.25 mM Probenecid (Sigma) in 500 μl of RPMI medium containing 10% FBS and 1% chiken serum for 60 min at 37°C. Then cells were washed several times with Ca^{2+}-free Tyrode buffer. Before Ca^{2+} measurement, cells were pretreated with Tyrode buffer containing 0.5 mM EGTA (Sigma). Cells were treated with 10 μM thapsigargin (TG; Sigma) for 300 s, then the extracellular Ca^{2+} concentration was restored to 2 mM. Changes in fluorescence intensity were monitored using FACS Calibur (BD, Tokyo, Japan).

IDENTIFICATION OF STIM1-ASSOCIATED MOLECULES

After 293T cells were transfected with STIM1(Full)-FLAG, the cells were lysed with lysis buffer (1% digitonin was used as a detergent), and subject to immunoprecipitation with ANTI-Flag® M2-Agarose Affinity Gel for over night at 4°C. The immunoprecipitated proteins were separated by electrophoresis on 5–20% SDS–polyacrylamide gels. Then, proteins on the gels were visualized with silver-staining (Wako, Osaka, Japan) according to manufacturer protocols.

After the completion of staining, the bands of interest were excised from the gel and digested with TrypsinGold (Promega). The digested samples were analyzed by nanocapillary reversed-phase LC-MS/MS using a C18 column (φ 75 μm) on a nanoLC system (Ultimate, LC Packing, Kent City, MI) coupled to a quadrupole time-of-flight mass spectrometer (QTOF Ultima, Waters, Milford, MA). Direct injection data-dependent acquisition was performed using one MS channel for every three MS/MS channels and a dynamic exclusion for selected ions. Proteins were identified by database searching (Mascot Daemon, Matrix Science, Boston, MA). Search parameters were as follows: MS tolerance of 0.2, MS/MS tolerance of 0.4 Da, protease specificity allowing for one missed cleavage site, fixed modification of carbamidomethylation of cysteine residues.

RESULTS

THE CYTOPLASMIC REGION OF STIM1 IS ESSENTIAL FOR ITS LOCALIZATION IN ER

Because STIM1 does not have a typical ER-retention sequence [Soboloff et al., 2006b; Baba and Kurosaki, 2009], it is a riddle that STIM1 mainly localizes in ER. To analyze the peculiar manner of its intracellular distribution, we constructed a series of deletion mutants as illustrated in Figure 1A. HeLa cells were transfected with each plasmid of STIM1(EX, EX + TM, EX + TM + CC, Full)-FLAG, and the protein synthesis was confirmed with Western blot using anti-FLAG antibody. Each deletion mutant protein was detected at the predicted sizes although the band for a mutant deleted both transmembrane and cytoplasmic domains was very faint (Fig. 1B, lower panel). We then analyzed protein trafficking of each mutant. After the transfection of plasmids into HeLa cells, their supernatant and cell lysates were prepared and subjected to Western blot. A specific band was detected in supernatant of HeLa cells transfected with STIM1(EX)-FLAG, but the bands for other transfectants is not clearly detected (Fig. 1B, upper panel). After surface proteins on each transfectant were labeled with biotin, the cell lysates were analyzed with Western blot using HRP-streptavidin or anti-FLAG antibody. As shown in Figure 1C, all STIM1 mutants excluding STIM1(EX) were efficiently expressed (detected by anti-FLAG antibody), but only STIM1(EX + TM) was massively expressed on the cell surface (detected by HRP-avidin). In addition, surface expressed STIM1(EX + TM + CC) was only faintly detected similar to STIM1(Full). These results indicate that the cytoplasmic segment (AA 246-593) containing the coiled-coil domains may determine the intracellular distribution of STIM1. In other words, STIM1 lacking its cytoplasmic region is likely to traffic from ER to golgi apparatus, resulting in the surface expression or secretion. In contrast, STIM1 with its cytoplasmic region tends to be restored in cytoplasm. This possibility was confirmed by experiments with a confocal microscopy. When STIM1(EX) lacking a transmembrane domain was expressed, only small amount of the protein was detected (Fig. 2), confirming that it was secreted as shown in Figure 1B. The other mutants, STIM1(Full) and STIM1(EX + TM + CC), were restored in ER, which was oriented by PDI-staining. In contrast, the distribution of STIM1(EX + TM) was not restricted to ER. Similar distribution patterns of STIM1 mutants were also observed in 293T cells (data not shown). Therefore, the coiled-coil domains of STIM1 critically contribute to its localization in ER where STIM1 mainly works as a Ca^{2+}-sensor.

THE CYTOPLASMIC REGION OF STIM1 YIELDS ITS PROTEIN STABILITY

Figure 2 showed that HeLa cells transfected with STIM1(Full)-FLAG and STIM1(EX + TM + CC)-FLAG, but not those with STIM1(EX + TM)-FLAG, changed the shape of ER to "the distended form," where STIM1 proteins seemed to be massively accumulated in ER. This might indicate that the cytoplasmic region corresponding to the coiled-coil domains has some specific effects, such as STIM1-stabilization. To clarify this possibility, we analyzed a half-life of each STIM1 mutant. After the transfection of plasmids for the deletion mutants into HeLa cells, the newly synthesized proteins were labeled with ^{35}S-methionin. The cells were lysed and subjected to immunoprecipitation using anti-FLAG antibody after the indicated periods of cultures. As shown in Figure 3, the half-life of STIM1(Full) was approximately 19 h. Although STIM1(EX + TM + CC) exhibited similar half-life to STIM1(Full), STIM1(EX + TM) disappeared more rapidly. Similar results were obtained in 293T cells as well as HeLa cells (data not shown). Therefore, the coiled-coil domains have an ability to stabilize STIM1 proteins.

THE CYTOPLASMIC REGION OF STIM1 IS ESSENTIAL FOR ACTIVATING SOCE

To validate physiological roles of cytoplasmic region of STIM1 in activating SOCE, we established STIM1-deficient DT40 B cells stably expressing STIM1(Full) and STIM1(EX + TM) (Fig. 4A), and examined whether these stably transfected cells have an ability to restore SOCE. As shown in Figure 4B, the reconstitution of SOCE was observed in DT40 cells expressing STIM1(Full), but not in those expressing STIM1(EX + TM). This data indicate that cytoplasmic region of STIM1 is essential for activating SOCE.

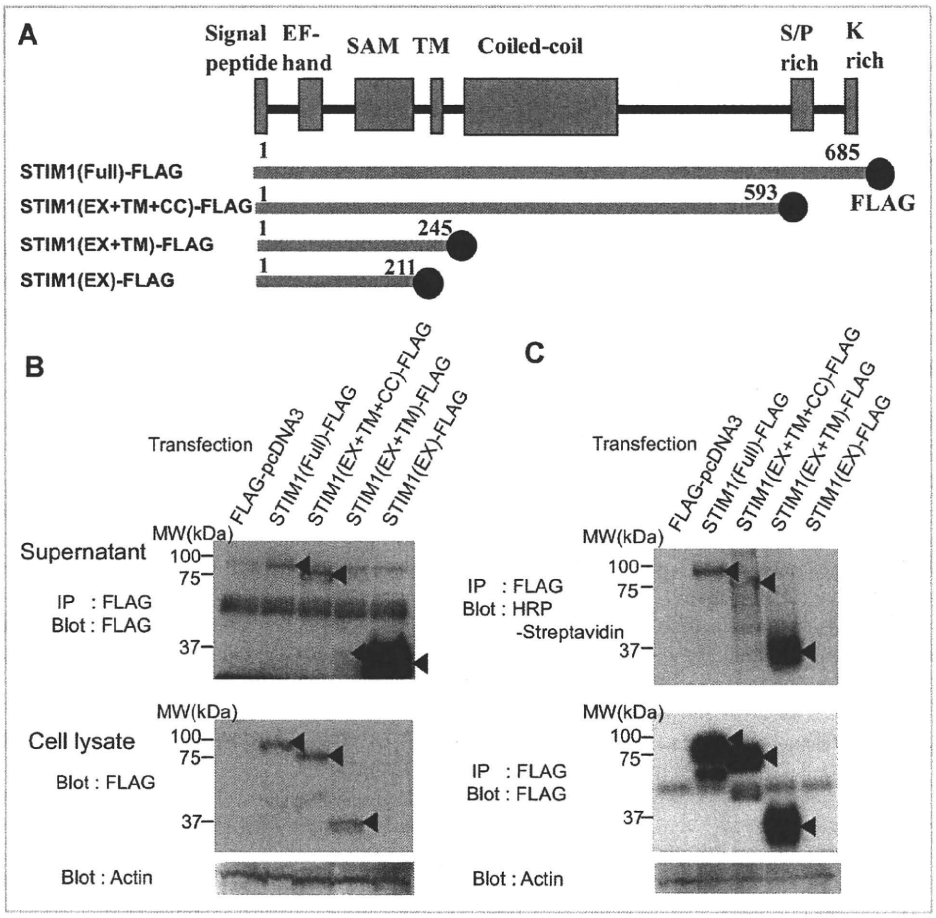

Fig. 1. The coiled-coil domains of STIM1 contribute ER-retention. A: Schematic representation of STIM1 functional domains and STIM1 mutants. TM, transmembrane domain; S/P rich, Ser/Thr-rich domains; K rich, Lysine-rich C-terminal domain. B: HeLa cells were transfected with the indicated STIM1 mutant expression plasmids, and their supernatant and cell lysates were collected after 24 h of cultures. Each supernatant was precipitated with ANTI-FLAG® M2-Agarose Affinity Gel. The precipitates as well as cell lysates were subjected to Western blot using an anti-FLAG antibody. One representative of three independent experiments is shown. Specific bands for each STIM1 mutant were shown by arrows. The membrane was deprobed and stained with anti-actin antibody for a loading control. C: Twenty-four hours after transient transfection of the indicated STIM1 mutant expression plasmids to HeLa cells, their cell surface proteins were biotinylated. Then, the biotin-labeled HeLa cells were lysed, precipitated with ANTI-FLAG® M2-Agarose Affinity Gel, and Western blotted with anti-FLAG and HRP-streptavidin. Specific bands for each STIM1 mutant were shown by arrow heads. The membrane was deprobed and stained with anti-actin antibody for a loading control. Similar results were obtained in three independent experiments.

IDENTIFICATION OF STIM1-ASSOCIATED PROTEINS

In the present study, we showed essential roles of the coiled-coil domains in the ER-retention as well as the protein-stabilization of STIM1. We also indicated that cytoplasmic regions of STIM1 are critical for activating SOCE. Recent reports have suggested that the C-terminal region of STIM1 is critical for the binding to the CRAC activating domain of Orai1 [Park et al., 2009; Yuan et al., 2009]. Other reports also indicated that the polybasic C-termini of STIM1 binds to calmodulin [Bauer et al., 2008] and that the short polypeptide motif (SxIP) of STIM1 associates with the microtubule-plus-end-tracking protein end binding protein-1 (EB1) [Honnappa et al., 2009]. Thus, it is likely that STIM1 may associate with several proteins, which modulate functions and/or protein characteristics of STIM1. To identify STIM1 associated molecules comprehensively, we performed co-immunoprecipitation experiments combined with mass spectrometry. After 293T cells were transfected with STIM1(Full)-FLAG or the empty FLAG-pcDNA3 plasmid, the cell lysates from each transfectant were prepared and subjected to immunoprecipitation with anti-FLAG antibody. When the immunoprecipitated proteins in the gel were visualized with silver staining, several specific bands were detected in the lane for the STIM1(Full)-transfected samples (Fig. 5A). Each specific band was then digested in gel with trypsin and subjected to LC-MS/MS analysis. As shown in Figure 5B, the approximately 80–90 kDa band (band 2) contains STIM1 in all experiments. Of importance, calnexin, which acts as a chaperone protein and exists in ER [Ni and Lee, 2007; Caramelo and Parodi, 2008], was always identified in the band 2 at a high score. Exportin1, transportin1, and